

SCIENCE & TECHNOLOGY

Journal homepage: http://www.pertanika.upm.edu.my/

Performance Evaluation of Jatropha Polyurethane Membrane Modified with Bio-based Carbon Dots for Pb(II) Removal

Umar Adam Majid¹, Zurina Zainal Abidin^{1,2*}, Nur Haninah Harun¹ and Khairul Faezah Md Yunos³

- ¹Department of Chemical and Environmental Engineering, Faculty of Engineering, Universiti Putra Malaysia, 43400 Serdang, Selangor, Malaysia
- ²Institute of Tropical Forestry and Forest Products, Universiti Putra Malaysia, 43400 Serdang, Selangor, Malaysia
- ³Department of Process and Food Engineering, Faculty of Engineering, Universiti Putra Malaysia, 43400 Serdang, Selangor, Malaysia

ABSTRACT

The filtration efficiency of the jatropha polyurethane (JPU) membrane, enhanced with bio-based carbon dots (CDs) derived from oil palm empty fruit bunch carboxymethylcellulose, was evaluated for real-world applications, specifically for the removal of lead (Pb(II)) ions. Using a central composite design (CCD) within response surface methodology (RSM), the parameters for JPU/CD membranes with a 0.65 wt% carbon-dot loading were investigated and optimized. Pressure of range 1.5-2.5 bar, feed concentration from 100 to 200 ppm, and solution from pH (9 to 13 were fed into the RSM. An optimum Pb(II) ion removal of 82% was predicted at conditions of pH 11, 135 ppm, and 2 bar, while the validated experimental result recorded 67% Pb(II) ion removal. A statistically non-significant term was excluded from the analysis through backward elimination to improve the model's accuracy. The quadratic regression model was significant ($R^2 = 0.90$) for the optimization prediction. Therefore, the results from the reduction model implied a satisfactory membrane

ARTICLE INFO

Article history: Received: 28 March 2025 Accepted: 18 May 2025 Published: 14 October 2025

DOI: https://doi.org/10.47836/pjst.33.6.16

E-mail addresses: umaradammajid@gmail.com (Umar Adam Majid) zurina@upm.edu.my (Zurina Zainal Abidin) nurhaninahharun@gmail.com (Nur Haninah Harun) kfaezah@upm.edu.my (Khairul Faezah Md Yunos)

* Corresponding author

performance, offering a better prediction for Pb(II) ions removal. The addition of CDs alters the membrane structure and properties, leading to improved water permeability and Pb(II) rejection, and positioning the bio-based JPU/CDs membrane as a promising sustainable solution.

Keywords: Carbon dots, filtration, heavy metals, Jatropha, membrane, vegetable oil

INTRODUCTION

Water resources are important for humans as water is a basic necessity for existence. The sudden exponential growth of the human population, along with industry advancement, affects the demand for freshwater reserves. For instance, in Malaysia, the demand for freshwater was projected to increase from 15,285 m³/d in 2010 to 20,338 m³/d in 2020, and the freshwater reserves per capita per day are decreasing at 5.8% per year, resulting in a projection that it to be diminished (Low et al., 2016). In addition, heavy metal contamination in water sources has become a health and environmental concern due to its persistence and toxicity. Pb(II) ions are highly toxic even at low concentrations, posing serious risks to aquatic ecosystems and human health. Sources of Pb(II) pollution include industrial discharge, mining activities, battery production, and metal plating processes (Fang et al., 2022; Wan Yaacob et al., 2009; van der Kuijp et al., 2013). Conventional methods for Pb(II) removal, such as ion exchange, chemical precipitation, and adsorption, often incur high operational costs with limited efficiency and secondary waste production. As a result, membrane-based filtration systems have gained attention as an effective water purification method due to their high selectivity and energy efficiency.

Membrane filtration systems have emerged as a key technology in water and wastewater treatment, offering efficient and environmentally friendly solutions for contaminant removal. These systems operate based on selective permeability, allowing water molecules to pass through while retaining suspended solids, pathogens, and dissolved contaminants such as heavy metals and organic compounds. Additionally, membrane processes are scalable, making them suitable for both small-scale applications and large industrial systems. One advanced configuration commonly employed is the crossflow filtration system, in which the feed water flows tangentially across the membrane surface rather than directly through it. This design significantly reduces fouling by minimizing the buildup of retained particles on the membrane, enhancing both operational efficiency and membrane lifespan (Poerio et al., 2022). The shear force generated by the crossflow also helps maintain a stable permeate flux, making it ideal for long-term continuous operation.

In addition, recent advancements in bio-based membranes have provided promising solutions for removing heavy metals, emphasizing both sustainability and cost-effectiveness. Successful fabrication of green sustainable biomaterials, such as those from cellulose, vegetable oil, and others, has heightened the interest (Idress et al., 2021; Marlina et al., 2017). Jatropha oil, a renewable and biodegradable resource, has emerged as a suitable precursor for polyurethane membrane synthesis due to its high hydroxyl content and compatibility with polymerization processes. Previous work by Harun et al. (2020) reported successful synthesis of bio-based membrane from jatropha oil with and without graphene oxide (GO) and its applications for filtration (Harun et al., 2022). However, this work needs further investigation to provide an insightful understanding of

the role of additives in tailoring the properties of the synthesis of bio-based membranes. Furthermore, optimizing membrane performance for efficient heavy metal removal remains a challenge, necessitating modifications that enhance adsorption capacity, permeability, and mechanical stability.

Nanomaterials like CDs have demonstrated excellent physicochemical properties, including high surface area, tunable functional groups, and superior adsorption capabilities (Gao, 2019). Integrating CDs as additives into polymer membranes has shown potential in improving heavy metal ion removal through enhanced surface interactions and increased hydrophilicity (Harun et al., 2020; Sgreccia et al., 2024).

In this study, JPU membrane was modified with bio-based CDs derived from the carbonization of oil palm empty fruit bunch (EFB) carboxymethylcellulose (CMC). The aim here was to assess its effectiveness in removing pollutants, particularly Pb(II) removal. This research employs a central composite design (CCD) within the RSM framework to investigate the effects of key process variables, namely feed concentration, operating pressure, and pH, on Pb(II) removal performance. The findings are significant to the growing field of bio-based membrane technology and offer a sustainable approach to removing heavy metals from aqueous solutions.

MATERIALS AND METHODS

Materials and Reagents

Crude jatropha oil (CJO) and CMC of oil palm EFBs were purchased from Bionas Sdn. Bhd. (Malaysia) and Waris Nova Cove Company (Malaysia), respectively. Glacial acetic acid was obtained from Fisher Scientific (Malaysia), while Amberlite™ IR-120, hexamethylene diisocyanate (HDI), and 30% hydrogen peroxide (H₂O₂) were supplied by Sigma-Aldrich (Malaysia). Sodium carbonate (Na₂CO₃), Lead nitrate (Pb(NO₃)₂), and methanol were obtained from R&M Chemicals (Malaysia). Lastly, anhydrous sodium sulfate (Na₂SO₄) was attained from PC Laboratory Reagent (Malaysia).

Synthesis of CDs

The method for producing CDs followed the process obtained from Issa, Abidin, Pudza, et al. (2020). An amount of 0.2 g of fine CMC was mixed with 30ml of polyethylene glycol (PEG, Sigma-Aldrich, Malaysia, 400 of molar mass 380-420 g/mol) (Sigma-Aldrich, Malaysia). The mixture was dissolved in 25 ml of deionized water and placed into a Teflon-lined stainless steel reactor, which was then tightly sealed. The reactor was then placed in an oven (ECOCELL®, MMM Group, Germany) and heated to 270°C for 6 hr to facilitate hydrothermal reactions. Subsequently, the liquid was cooled to room temperature and centrifuged (Biosan LMC-3000, Fischer Scientific, Latvia) at 11,200 × g for 15 min.

Finally, the mixture was filtered through a 2 μ m Whatman filter paper to isolate the CDs from the remaining components.

Synthesis of Epoxidized Jatropha Oil (EJO), Jatropha Oil-based Polyol (JOL), JPU/CDs Membrane

EJO was synthesized via an epoxidation reaction following a previously reported method (Harun et al., 2020). CJO and glacial acetic acid were mixed in a 1 L reaction flask, with AmberliteTM IR-120 ion-exchange resin added as a catalyst at 16 wt% relative to CJO. The reaction mixture was heated to 65°C in a water bath under continuous stirring at 900 rpm. Once the temperature stabilized, 30% H₂O₂ was gradually introduced in a dropwise manner, maintaining a molar ratio of 6:1:1.7 of glacial acetic acid, carbon double bond (C=C), and H₂O₂. The temperature subsequently increased to 75°C and was maintained for 5 hr to ensure complete epoxidation. Following the reaction, the catalyst was removed, and the mixture was quenched with excess water in three consecutive cycles at 90, 20, and 90°C, respectively, facilitating efficient acid removal. The separation process resulted in the formation of two distinct layers: an upper epoxy-rich layer and a lower aqueous phase, which was discarded at the end of each cycle. To remove residual moisture, Na₂SO₄ was added at a 1:0.15 (m/m) ratio, and the mixture was dried at 80°C for 12 hr. The dried solid desiccant was then separated by decantation, yielding the final EJO product.

The obtained EJO underwent ring-opening hydrolysis to produce JOL. In a 1 L reaction flask, water (10% of the EJO weight), methanol (5:1 ratio to water), and sulfuric acid (0.3% of the total reaction mixture) were combined and heated to 64°C under continuous stirring at 800 rpm. Once the reaction temperature was stabilized, 100 g of EJO was added, and the reaction proceeded for 30 minutes. To neutralize the reaction, Na₂CO₃ was introduced, and the mixture was allowed to cool. The resulting polyol phase was separated by discarding the precipitate. Residual water and methanol were subsequently removed through vacuum evaporation at 45°C, continuing until the final JOL product was obtained, confirmed by the absence of visible aqueous residues.

CDs were incorporated into jatropha-based polymer membranes by dispersing CDs into the JOL solution using a Branson M1800 sonicator (SonicsOnline, USA). Based on preliminary screening, only the JPU/CDs membrane with 0.65 wt% CD loadings was subjected to detailed filtration evaluation. To make JPU, HDI was introduced into the mixture in a 5:5 (v/v) ratio with JOL (Harun et al., 2020). The reaction mixture was stirred at 600 rpm while maintaining a temperature range of 90–100°C for 1 hr to ensure homogeneous mixing and polymerization. The resulting solution was cast onto a glass Petri dish, forming a membrane layer with a thickness of 0.5 mm, as measured using a caliper. The membrane was then subjected to thermal curing in an oven (ECOCELL®, MMM Group, Germany) at 150°C for 8 hr. Upon completion of the curing process, the

JPU/CDs composite membrane was carefully exfoliated from the Petri dish using a spatula and used in filtration.

Filtration Method

A crossflow system was used to perform the filtration process to test the JPU/CDs (0.65 wt%) membrane. The results from the filtration process were analyzed using inductively coupled plasma optical emission spectroscopy (ICP-OES, Optima 7300 DV PerkinElmer, USA) to measure the amount of remaining Pb(II) after the filtration. Results obtained from the ICP were then computed to determine the flux (Jw) and the amount of Pb(II) ions rejected (R), using Equations 1 and 2.

$$J_w = \frac{V}{A \cdot \Delta t} \tag{1}$$

where V is the permeate (L), A is the effective surface area (m²), J_w is the water flux (L/m².h), and t is the time taken for filtration (min).

$$R = \left(1 - \frac{C_p}{C_f}\right) \times 100\% \tag{2}$$

where C_p and C_f are the Pb(II) ion concentrations in the permeate and the feed, respectively.

Screening Parametric by Single Factor Experiment Studies

In this experiment, preliminary screening was conducted to determine the appropriate range of factors that influence the experiments, which was essential to decide the best range to be entered in RSM. Three different factors, acidity, pressure, and concentration, were tested to find the optimal conditions, with the corresponding studied ranges of 100–250 ppm, 1.5–2.5 bar, and pH 9–13, respectively. The tests examined the effects of each component on the removal of Pb(II) ions, varying one factor at a time (OFAT), within their corresponding parameter ranges. Then, based on these results, the ranges were verified to be appropriate for optimization studies.

Optimization by RSM

Pb(II) ion feed concentration, solution pH, and pressure were three independent variables, used in RSM to create and optimize the experimental design for optimizing Pb(II) removal from the aqueous solution (Table 1) and the interaction between variables. From the CCD, 17 trial experiments were performed, with three repetitions at the center points. The CCD

was used to reduce the number of experiments, as it can gather information on data fitting with fewer experimental trials for the optimization process (Chee et al., 2021; Harun et al., 2022).

Table 1
RSM experimental design for Pb(II) removal using JPU/CDs 0.65 wt% membrane

Symbol	Parameters	Low	High
X_1	Concentration (ppm)	100	200
X_2	Pressure (bar)	1.5	2.5
X_3	Acidity (pH)	9	13

Note. RSM = Response surface methodology; Pb(II) = Lead ions; JPU = Jatropha polyurethane; CDs = Carbon dots; X_1 = Concentration; X_2 = Pressure; X_3 = Acidity

Then the response was fitted into a second-order polynomial model, as shown in Equation 3:

$$y = \beta_0 + \sum_{i=1}^k \beta_i x_i + \sum_{i=1}^k \beta_{ii} x_i^2 + \sum_{i=1}^k \sum_{j=i+1}^{k-1} \beta_{ij} x_i x_j$$
 [3]

where y is the dependent variable (Pb(II) rejection); x_i and x_j are the independent variables that influence the response y; β_0 , β_i , β_{ii} , and β_{ij} are the coefficients of intercept, linear term, quadratic term, and interaction, respectively, and k is the number of variables. In this case, k = 2.

Determination of Zeta Potential at Different Solution pH Values

A particle size analyzer, Zetasizer (LA-960V2, HORIBA, Japan), was used to measure the zeta potential of the sample. The solution pH was adjusted from 9 to 13 using sodium hydroxide (NaOH, 1.0 mol/L, Sigma-Aldrich, Malaysia). The zeta potential, which arises as an electrical double layer developed at the solid—liquid interface, describes the surface charge of a membrane. It is influenced by the functional groups on the membrane surface, the ions in the feed solution, and the pH (Deshmukh & Childress, 2001; Hu et al., 2023).

RESULTS AND DISCUSSION

Screening Factors by OFAT Experiments

Preliminary screening through OFAT was conducted to determine the range of parameters affecting the performance of Pb(II) removal. These ranges served as a feeder for the subsequent optimization work using RSM. The range of values studied was as follows:

(a) feed concentration (100, 150, 200, and 250 ppm); (b) water pressure (1, 1.5, 2.0, and 2.5 bar); and (c) pH values (3, 4, 5, 9, 11, and 13).

Effect of Feed Concentration on Pb(II) Rejection

In studying the effect of feed concentration, experiments were conducted at a constant pH of 7 and a pressure of 1.5 bar. Based on the results obtained, as shown in Figure 1, the rejection trend initially increased until it reached a peak of 32% at 150 ppm, and then decreased as the initial feed concentration was further increased. This may be explained by changes in membrane charge density that can be affected by the bulk ion concentration. This influences both the selective ion adsorption on the top membrane surface and within the pore. The build-up of ions near the membrane surface increases the membrane charge density and thus increases the rejection of Pb(II). However, the excess concentration of solute on the surface of the membrane can repulse the solvent from passing through the membrane. This scenario can be attributed to concentration polarization, in which the solute accumulates at the membrane surface, thereby increasing the local osmotic pressure and reducing Pb(II) rejection (Idress et al., 2021). Hence, the 100 to 200 ppm concentration range was selected for implementation in the optimization using RSM.

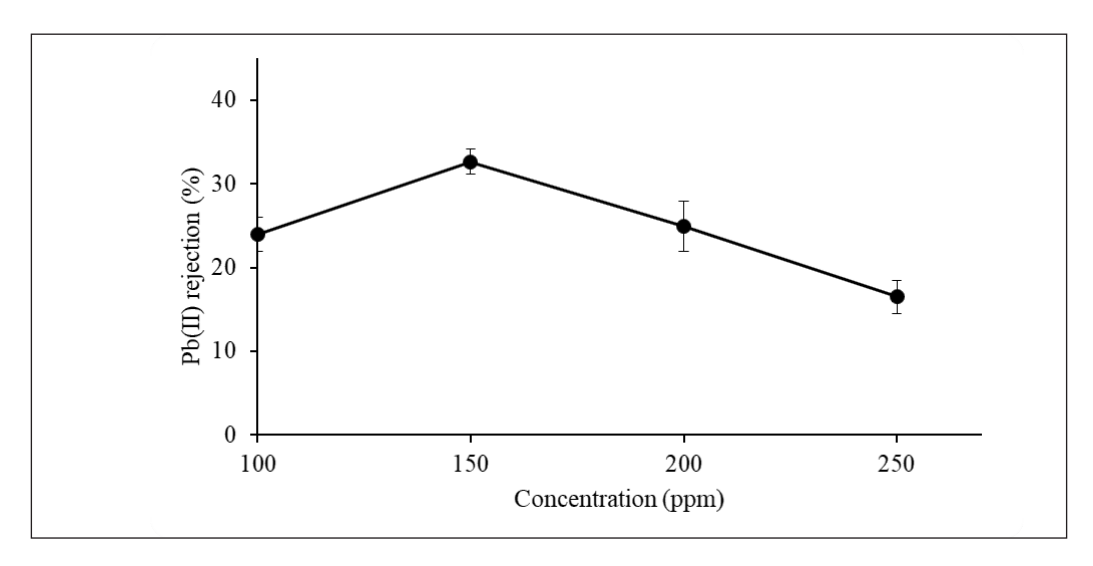


Figure 1. The lead ions (Pb(II)) rejection at different feed concentrations

Effect of Feed Pressure on Pb(II) Rejection

For studying the effect of pressure, the value was tested from 1 to 2.5 bar with an increment of 0.5 bar at a constant feed concentration of 100 ppm and pH 7. The rejection of Pb(II) increased as the pressure increased, reaching its highest value at 2.5 bar (Figure 2). The peak of the rejection was not found due to the system operation constraints and limitations.

Therefore, the pressure range of 1.5–2.5 bar was used in the following optimization process. High pressure exerts more force to carry solute to the membrane surface and causes solute accumulation on the membrane surface, which may contribute to concentration polarization (Emamjomeh et al., 2019). Meanwhile, the increased variability observed in the error bars at higher operating pressures (2.0 and 2.5 bar) can be attributed to intense mechanical stress on the membrane, potentially causing minor structural shifts or compaction, which can lead to inconsistent flow rates and separation performance (Stade et al., 2013). It may also be due to the inherent randomness and heterogeneity of the bio-based material used in membrane fabrication (Morales-Jiménez et al., 2023).

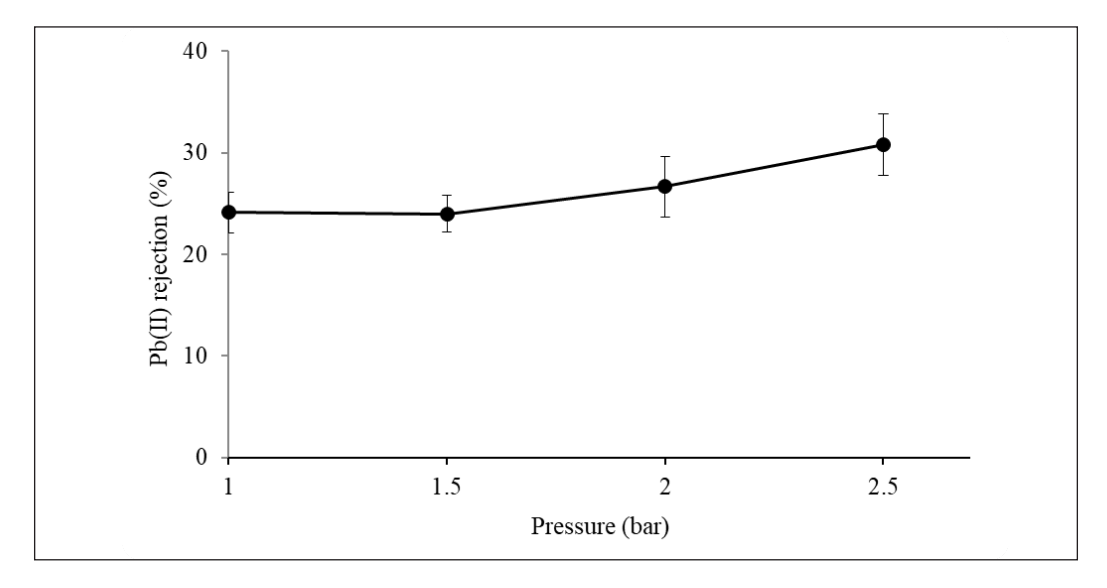
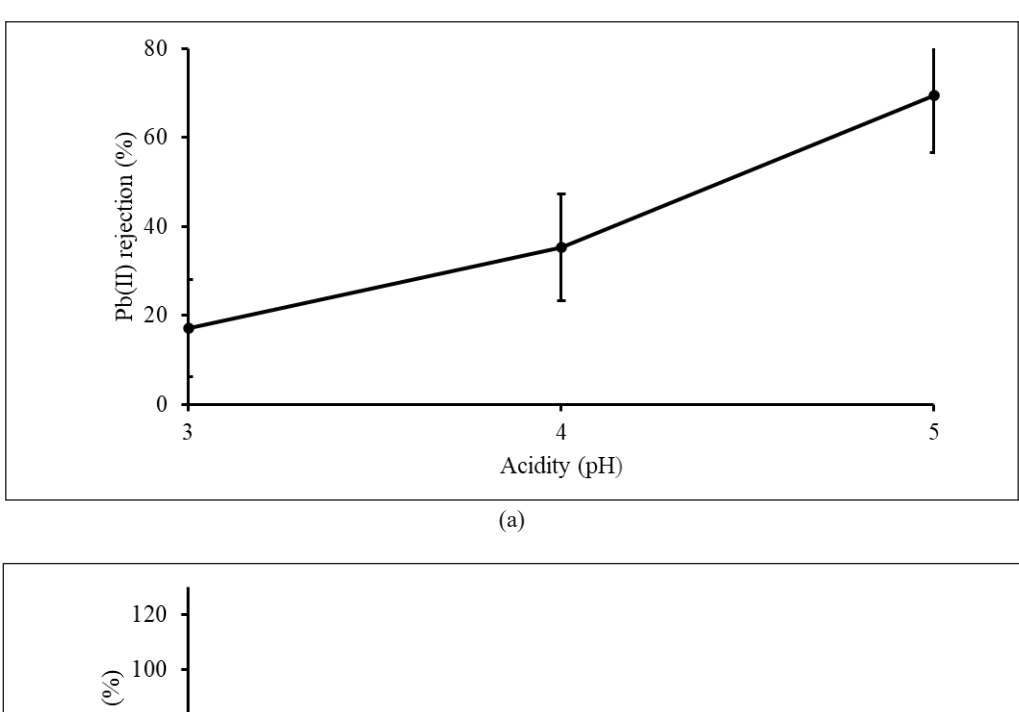


Figure 2. The lead ions (Pb(II)) rejection at different feed pressures

Effect of Solution pH on Pb(II) Rejection

A constant pressure of 1.5 bar and a feed concentration of 100 ppm were selected to investigate the effect of pH. The investigation in acidic conditions was conducted from pH 3 to pH 5, showing an increment from 17 to 69% rejection at pH 3 and pH 5, respectively, with no optimum peak observed (Figure 3a). Further testing in basic conditions showed an increase in the rejection from pH 9 to pH 11, and started to decrease at pH 13. The optimum peak was only found at pH 11 at 76% rejection (Figure 3b). Although the error bars at pH 4 and 5 may appear more prominent visually, the standard deviations at pH 3, 4, and 5 are relatively similar, ranging from approximately 11 to 13%. This indicates that the variability in measurements across these pH values is consistent and within an acceptable range. The apparent difference in error bar size is not due to increased variability at specific pH levels but rather sometimes reflects the normal fluctuation expected from the use of bio-based

membrane materials, which can exhibit minor structural or compositional differences across samples. pH values ranging from 6 to 8 were excluded from this study, as operating near neutrality better reflects natural waters and minimizes charge-related interferences that can compromise membrane performance. Previous work has shown that polymer membranes perform most effectively under strongly acidic or basic conditions, where surface charges are maximized (Harun et al., 2022; Khamis et al., 2023). In the near neutral range (pH 6–8), however, the zeta potential approaches the membrane's isoelectric point, lowering surface-charge density and, consequently, diminishing electrostatic interactions with Pb(II) ions (Duclos-Orsello et al., 2004).



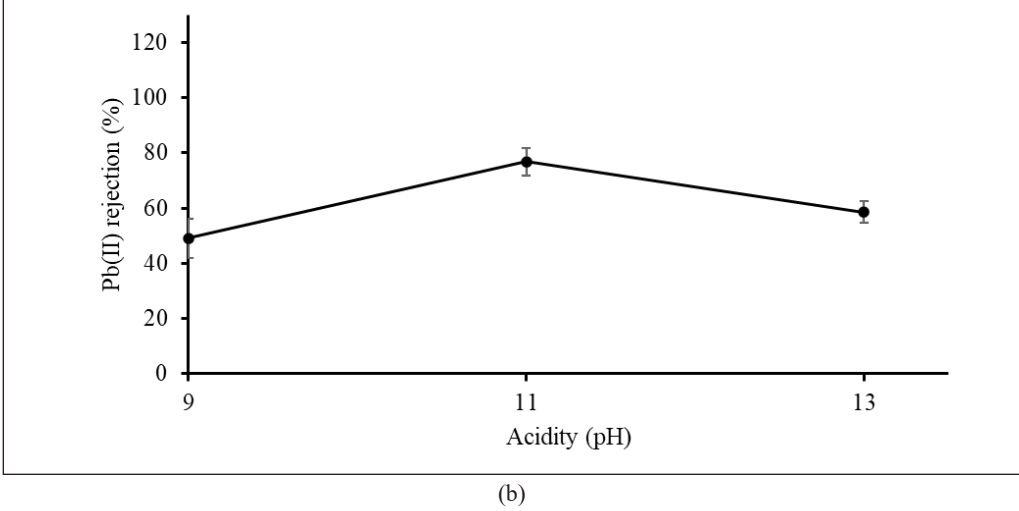


Figure 3. The Pb(II) rejection at (a) acidic and (b) basic conditions, respectively

Because pH alters the membrane's surface-charge density and thus its zeta potential, the filtration mechanism and overall efficiency are correspondingly affected. To clarify this relationship, the zeta potential of the JPU/CDs membrane in both distilled water and an aqueous Pb(II) solution across the relevant pH range was measured. As shown in Figure 4, the JPU/CDs 0.65 wt% membrane in distilled water exhibits a negative zeta potential of -41, -32, and -32 mV at pH 9, pH 11, and pH 13, respectively. This indicates that the JPU/CDs membrane possesses a negatively charged surface under alkaline conditions. Generally, at high pH, the concentration of H⁺ ions decreases, leading to the deprotonation of functional groups such as hydroxyl (-OH) and carboxyl (-COOH), thereby increasing the negative charge on the membrane surface. Conversely, under low pH conditions, the abundance of H⁺ ions promotes protonation of these functional groups, resulting in a more positive surface charge. However, at pH 11 to 13, zeta potential started to plateau as the surface functional group has fully deprotonated, nearing surface saturation (Junker et al., 2023).

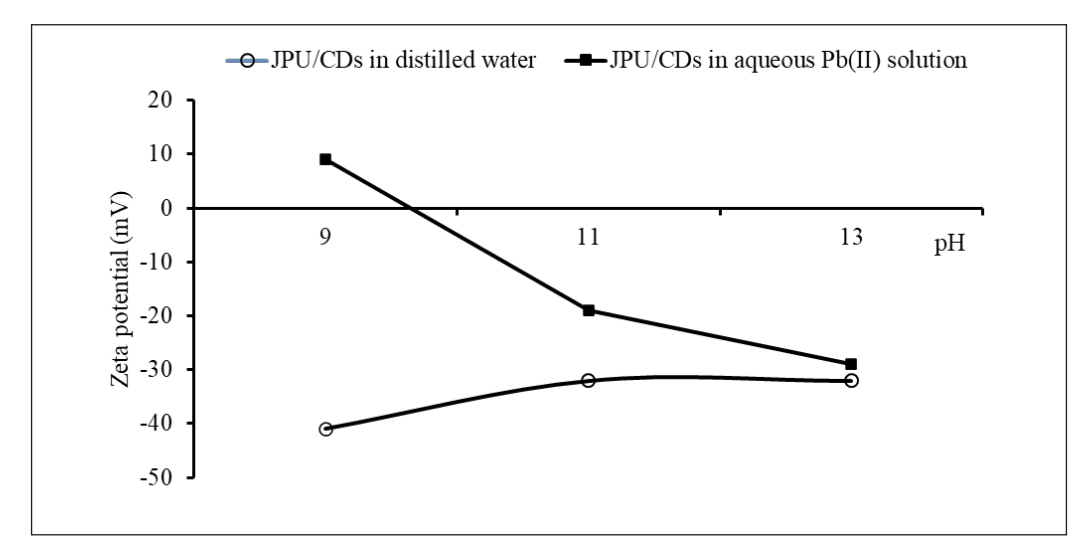


Figure 4. Zeta potential on jatropha polyurethane (JPU)/carbon dots (CDs) 0.65 wt% membrane at different pH levels in distilled water and in lead ions (Pb(II)) solution

In aqueous Pb(II) solution, the zeta potential values were measured to be 9, -19, and -29 mV at pH 9, pH 11, and pH 13, respectively. Notably, at pH 9, the value significantly shifted from -41 mV (in distilled water) to 9 mV (in Pb(II) solution). This can be attributed to the charge reversal caused by the adsorption of Pb(II) ions onto the negatively charged membrane surface. Under basic conditions, deprotonation of surface functional groups increases the negative surface charge density, facilitating strong electrostatic attraction between the membrane and lead (Pb²⁺) ions. As Pb²⁺ ions accumulate and bind to these sites, they effectively neutralize or even overcompensate for the negative charge, leading to a net positive zeta potential. (Figures 5 and 6).

As the pH increased, with the progressive addition of NaOH, the zeta potential changed back toward more negative values (-19 mV at pH 11 and -29 mV at pH 13). This trend suggests that at higher pH, Pb(II) ions may experience precipitation as lead hydroxide (Pb(OH)₂) and reduced electrostatic interactions with the membrane surface, thereby restoring the negative charge (Figures 5 and 6). Additionally, the presence of excess hydroxyl (OH⁻) ions may have contributed to charge repulsion effects, leading to a more negative zeta potential. However, at pH 13, the competition between Pb(II) and counter ions (such as sodium ions [Na+] and others) screens the negatively charged membrane surface, reducing the electrostatic attraction of Pb²⁺ and thereby lowering Pb(II) removal efficiency (Figure 6). This highlights the pH-dependent nature of the membrane's surface charge in the removal of heavy metals.

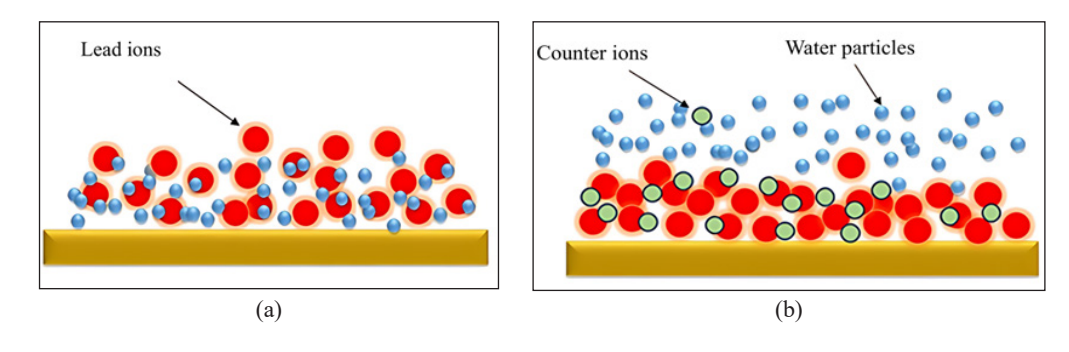


Figure 5. Illustration of the mechanisms where (a) favorable adsorption of lead ions (Pb(II)); (b) concentration polarization on the membrane surface

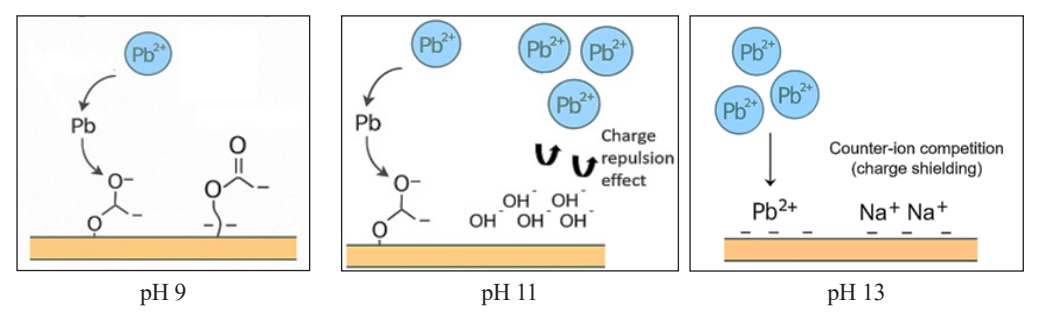


Figure 6. Schematic illustration of the possible binding mechanism at pH 9, pH 11, and pH 13, respectively *Note*. Pb^{2+} = Lead ions; OH = Hydroxide ions; Na^+ = Sodium ions

CDs have long been recognized as effective polymer modifiers, substantially enhancing physical, chemical, and thermal stability (Feng et al., 2021). These improvements impart the material with distinctive functional attributes, which in turn promote high rejection efficiencies for target compounds (Keçili et al., 2020). In addition, the presence of abundant

hydroxyl groups on CDs increases the membrane's hydrophilicity and adsorption capability, enabling stronger interactions with lead ions via hydrogen bonding or coordination (Petrović, 2008; Shabbir et al., 2023; Xia et al., 2023). The use of additives like CDs also modifies surface characteristics and pore structures, yielding a more uniform distribution of smaller pores that enhances the size exclusion of heavy metal ions (Cruz et al., 2023; Harun et al., 2022; Khdary et al., 2023; Xia et al., 2023). Altogether, these enhancements result in a membrane with superior rejection capabilities for heavy metals, especially Pb(II) ions in this study, and improved overall operational efficiency.

Membrane fouling is an inherent phenomenon in pressure-driven separations, inevitably diminishing filtration performance. While this study did not explicitly quantify fouling, the progressive decline in permeate flux serves as indirect evidence, indicating the increasing hydraulic resistance caused by solute deposition on or within the membrane during operation, as similarly reported by other studies (Abu-Zurayk et al., 2023). This accumulation is expected to impact long-term membrane performance by reducing available binding sites and potentially increasing filtration resistance. The retained contaminants are expected to contribute to progressive fouling of the filtration medium (Al-Rashdi et al., 2013; Shi et al., 2014; Zularisam et al., 2007). On the other hand, the improved hydrophilicity imparted by CDs' functional groups has been reported to facilitate better water permeability while reducing fouling, thus supporting sustained filtration performance (Mamba et al., 2021; Xia et al., 2023).

In short, based on OFAT studies, the suitable range for performing RSM optimization analysis was effectively determined to be as follows: feed concentration (100, 150, and 200 ppm), pressure (1.5, 2.0, and 2.5 bar), and pH values (9, 11, and 13).

Optimization of JPU/CDs Membrane Filtration

The experiment was further optimized by utilizing the OFAT findings, which were then fed into the RSM software to investigate the relationship between all the parameters. RSM software implemented a mathematical model (CCD) to minimize the amount of testing needed to achieve the output. The input parameters were feed concentration (ppm) (A), pressure (bar) (B), and acidity (pH) (C). The results are shown in Table 2.

Table 2
RSM simulation data when utilizing CCD and face-centered alpha

No.	Concentration (ppm)	Pressure (bar)	Acidity (pH)	Pb(II) rejection (%)
1	100	1.5	9	16
2	200	1.5	9	45
3	150	2	9	62
4	100	2.5	9	41

Table 2 (continue)

No.	Concentration (ppm)	Pressure (bar)	Acidity (pH)	Pb(II) rejection (%)
5	200	2.5	9	53
6	150	1.5	11	43
7	100	2	11	56
8	150	2	11	91
9	150	2	11	80
10	150	2	11	98
11	200	2	11	63
12	150	2.5	11	64
13	100	1.5	13	51
14	200	1.5	13	19
15	150	2	13	69
16	100	2.5	13	66
17	200	2.5	13	14

Note. RSM = Response surface methodology; CCD = Central composite design; Pb(II) = Lead ions

Model Fitting

Using RSM, experimental data were analyzed by fitting them into four different models: linear, two-factor interaction (2FI), quadratic, and cubic, to determine the regression equation. The models were evaluated based on the *F*-test value and *p*-value obtained from analysis of variance (ANOVA), as summarized in Table 3. The fitting process was based on polynomial models, including linear, quadratic, and cubic equations. In general, model selection was guided by the highest-order polynomial that was not aliased (Behera et al., 2018; Issa, Abidin, Sobri, et al., 2020).

Table 3
RSM response data using CCD using face-centered alpha

Source	Sum of squares	Df	Mean square	F-value	<i>p</i> -value Prob > <i>F</i>	Remarks
Mean	50996.37	1	50996.37	-	-	
Linear	534.83	3	178.28	0.27	0.8479	
2F1	2197.60	3	732.53	1.13	0.3827	
Quadratic	5594.76	3	1864.92	14.82	0.0020	Suggested
Cubic	199.86	4	49.97	0.22	0.9112	Aliased
Residual	681.18	3	227.06	-	-	
Total	60204.62	17	3541.45	-	-	

 $Note. \ RSM = Response \ surface \ methodology; \ CCD = Central \ composite \ design; \ Df = Degree \ of freedom; \ Prob = Probability; \ p-value < 0.05 \ denotes \ significance; \ The \ underline \ means \ quadratic \ is \ the \ most \ fitted \ and \ the \ selected \ model$

Additionally, to further assess model compatibility, the lack-of-fit (LOF) value was evaluated. The reliability of the model depends on the significance of the LOF value, which is influenced by midpoint replication. A model is considered reliable when the LOF value is non-significant (p-value > 0.005). Based on this assessment, the quadratic model, with a LOF value of 0.4061, was identified as the best fit for the experimental data and deemed non-significant.

ANOVA

To evaluate the significance of the fitted model, an ANOVA was conducted. As shown in Table 4, the coefficient of determination (R^2) for the predicted model is 0.9043, indicating a strong correlation between the experimental data and the model predictions. Since R^2 is close to 1, it suggests a good model fit. However, R^2 alone may not be a reliable measure

Table 4
RSM response data using CCD using face-centered alpha

Source	Sum of squares	Df	Mean square	F-value	<i>p</i> -value Prob > <i>F</i>	
Model	8327.197	9	925.244	7.351	0.008	
A - Concentration	130.287	1	130.287	1.035	0.343	
B - Pressure	403.528	1	403.528	3.206	0.116	
C - pH	1.01792	1	1.018	0.008	0.931	
AB	164.294	1	164.294	1.305	0.291	
AC	1966.542	1	1966.542	15.624	0.005	
BC	66.765	1	66.765	0.530	0.490	
A^2	604.735	1	604.735	4.805	0.065	
B^2	1108.574	1	1108.574	8.807	0.021	
\mathbb{C}^2	213.961	1	213.961	1.699	0.234	
Residual	881.047	7	125.864			
Lack of fit	715.297	5	143.059	1.726	0.406	
Pure error	165.750	2	82.875			
Cor total	9208.244	16				
Statistical analysis of the regression equation						
R-squared	0.904		Std. Dev.	11.22		
Adj R-squared	0.781		Mean	54.77		
Pred R-squared	0.579		CV%	20.48		
Adeq precision	8.189		PRESS	3870.81		

Note. RSM = Response surface methodology; CCD = Central composite design; Df = Degree of freedom; Prob = Probability; AB = Concentration-pressure; AC = Concentration-pH; BC = Pressure-pH; Adj R-squared = Adjusted R-squared; Pred R-squared = Predicted R-squared; Adeq precision = Adequate precision; Cor total = Corrected total; Std. Dev. = Standard deviation; CV = Coefficient of variance; PRESS = Residual error sum of squares

of model quality, as it can be artificially inflated by adding additional terms, regardless of their statistical significance.

To account for this limitation, adjusted R^2 (adj- R^2) and predicted R^2 (pred- R^2) provide more robust assessments of model performance (Halim et al., 2021). Adj- R^2 accounts for the number of predictors in the model, ensuring that only significant terms contribute meaningfully to the model. Meanwhile, predicted R^2 evaluates the model's predictive capability, helping to identify potential overfitting.

In this study, the adj- R^2 value of 0.7813 suggests that the model effectively describes the relationship between experimental data and model predictions. However, the pred- R^2 value of 0.5796 indicates a potential need for model refinement, as a lower pred- R^2 may suggest overfitting or the presence of non-significant terms that should be reconsidered. Therefore, further model optimization, such as reducing non-essential terms, may be necessary to improve its predictive accuracy.

In addition to that, the model's validity was improved based on other statistical characteristics such as adequate precision (Adeq precision), coefficient of variations (CV%), and residual error sum of squares (PRESS). The results of these data are shown above in Table 4. The Adeq precision assesses the signal-to-noise ratio that compares the range of the predicted values at the design points to the average prediction variance (Halim et al., 2021). That is, the ratio higher than 4 shows adequate model discrimination. The Adeq precision value obtained is 8.189, suggesting that the ratio is adequately accurate. In addition, the CV% value represents the degree of dispersion of the data points around the mean value. A lesser value (10%) indicates good reproducibility of the model. However, the obtained CV% from this model is 20.48. This shows the standard deviation is high relative to the mean. Apart from that, the PRESS value describes the model's capacity to fit each point in the design by fitting the model to all design points, excluding the predicted one (Halim et al., 2021). The residual values are then squared and added to yield the PRESS value reported in ANOVA. A lower value is preferred, indicating a high pred- R^2 score. However, the PRESS value generated from this is 3870.81, which is quite large, and can be associated with the low pred- R^2 value.

To further enhance the accuracy of the predicted model, additional steps were taken to eliminate a statistically non-significant term from the analysis using a reduction method. This process was carried out incrementally through backward elimination, starting with the least significant term, until a higher pred- R^2 value was achieved. The analysis revealed that removing terms with a p-value greater than 0.5 provided the best prediction for Pb(II) ion rejection. As a result of this reduction method, the pred- R^2 value improved to 0.8878 (88.78%), indicating strong predictive capability for the refined model.

Additionally, the adj- R^2 value saw a slight increase to 0.7941 (79.41%). The reduced model also showed improvements in the LOF and adequate precision, with values rising

to 0.438 and 8.532, respectively. Furthermore, the CV% and PRESS values decreased to 19.87% and 3572.71, respectively. These results demonstrate that the model's precision and predictive performance were enhanced. The final empirical models, after excluding the insignificant terms (BC) and (y), are presented in Equation 4. This equation highlights the inclusion of both linear effects and interactions between parameters for predicting Pb(II) ion rejection.

$$y = 80.83 - 3.61 (A) + 6.35 (B) + 0.32 (C) - 4.53 (AB) - 15.68 (AC) - 15.02 (A^2) - 20.34 (B^2) - 8.94 (C^2)$$
[4]

where A represents the feed concentration (ppm), B denotes pressure (bar), and C stands for the solution's pH value. A positive sign in the equation signifies a synergistic effect, whereas a negative sign reflects a resistive effect, based on the factors involved.

In the above equation, the coefficient of A (feed concentration) is -3.61, indicating that an increase in Pb(II) feed concentration negatively impacts removal efficiency. This can be attributed to saturation of adsorption sites on the membrane, where excessive Pb(II) ions exceed the membrane's capacity, reducing overall rejection. The coefficient of B (pressure) is +6.35, suggesting a positive correlation between pressure and Pb(II) removal. Increased pressure enhances convective mass transport, driving more Pb(II) ions toward the membrane and improving rejection efficiency through size exclusion and electrostatic repulsion. Finally, the coefficient of C (pH) is +0.32, indicating a minor positive effect of pH on Pb(II) removal. At higher pH, Pb(II) may form insoluble hydroxides (Pb(OH)₂), facilitating precipitation and improving removal. However, since the effect size is small, the membrane's role in rejection may dominate over precipitation.

The negative interaction between feed concentration and pressure (coefficient -4.53) implies that at higher Pb(II) concentrations, increased pressure does not proportionally enhance removal efficiency. This could be due to concentration polarization effects, where excessive Pb(II) ions accumulate near the membrane surface, creating a diffusion barrier that limits the process. The strong negative effect of the feed concentration—pH interaction (-15.68) suggests that increasing pH at higher Pb(II) concentrations significantly reduces removal efficiency. This may be due to Pb(II) complexation or increased ionic competition, which alters electrostatic interactions between Pb(II) and the membrane.

For the quadratic effect, the negative coefficient of -15.02 feed concentration $(A^2 = -15.02)$ indicates a nonlinear decrease in Pb(II) removal at higher concentrations. Beyond an optimal point, adsorption sites become overwhelmed, resulting in a sharp decline in removal efficiency. The strongest quadratic effect is observed for pressure $(B^2 = -20.34)$, suggesting that after an optimal pressure level, further increases reduce efficiency. This could be due to membrane compaction, which alters pore size and permeability, negatively

affecting Pb(II) rejection. Lastly, the negative quadratic effect of pH (C^2 = -8.94) implies that while moderate pH improves removal, excessive pH shifts the equilibrium towards Pb(II) precipitation rather than membrane adsorption, reducing effectiveness.

Residual Analysis

Residual analysis is used to evaluate the distribution of the residuals, normality, and presence of outliers (Nobre & da Motta Singer, 2007). To further investigate four diagnostic graphs, predicted responses versus observed responses, normal probability plot, residuals versus predicted responses, and residuals versus run order were examined as depicted in Figure 6. Based on the plots analyzed, from Figure 7a, the predicted response versus observed response shows that the prediction deviation does not deviate far from the normal

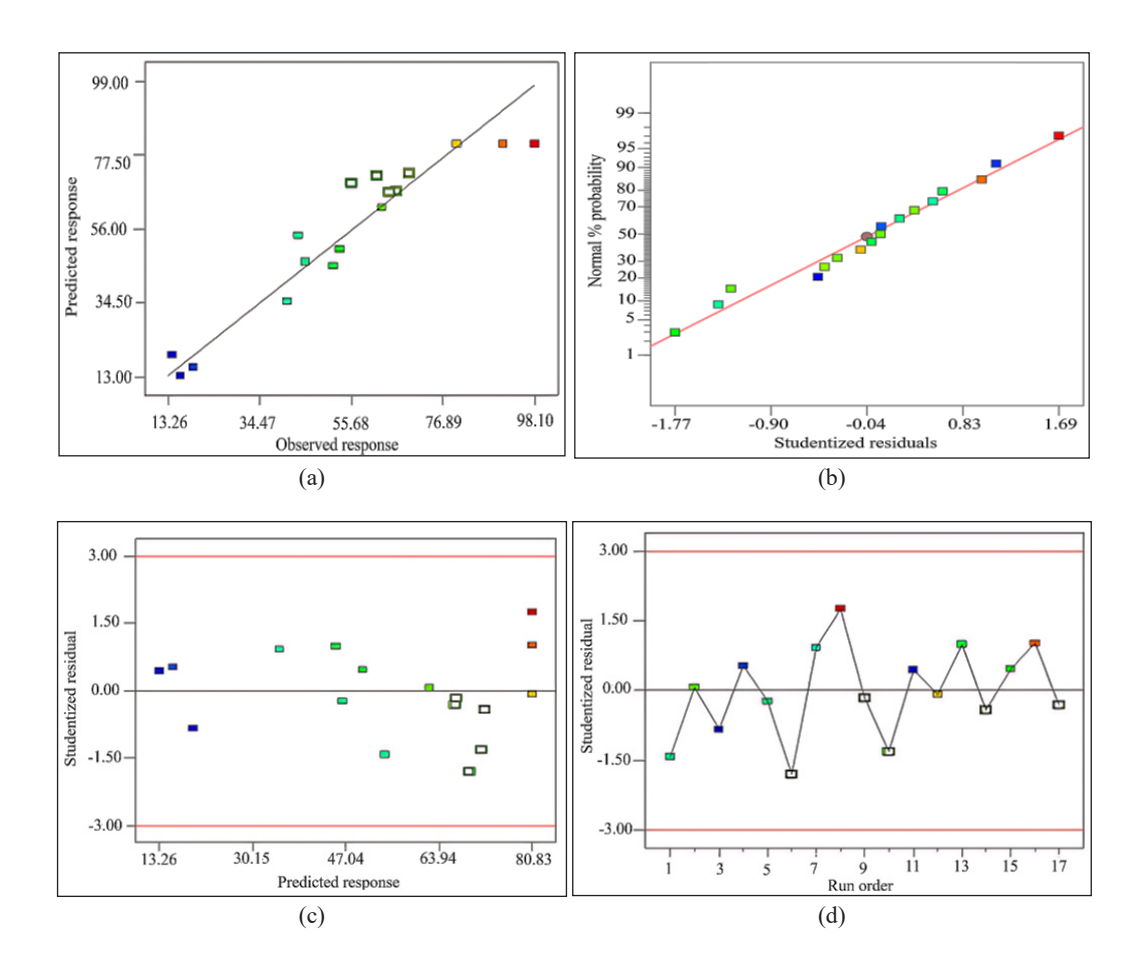


Figure 7. The residuals analysis diagnostic plots for (a) predicted against observed responses, (b) normal probability plot, (c) residuals against predicted responses, and (d) residuals against run order *Note*. Red lines refer to the studentized residual limits

line. On top of that, similar plotting can be seen in Figure 7b, which shows the validity of the ANOVA results (Tiwari et al., 2017). Apart from that, the residual plot versus predicted response shows the variance homogeneity based on the distribution of residual plots randomly on both sides of the normal line, which denotes the consistency of the variance (Halim et al., 2021). In addition to that, the scattered residual points from diagnostic plots in Figure 7c exhibit no outliers; that is, the residual points are only distributed randomly within the upper and lower limit lines (Vining, 2010). Similarly, the residuals plot versus run order, as shown in Figure 7d, shows residual plot inside the upper and lower limit lines, and residual points were scattered randomly about the normal line with no discernible patterns, indicating that the residuals are independent of one another and hence obey the ANOVA assumptions. The ANOVA assumptions were met because of the residuals analysis, and it can be said that the regression model produced unbiased coefficient estimates with minimum variance.

Effect of Filtration Factors Based on the Response Surface Plots Analysis

The interaction between the independent factors and the responses was visualized using response surface plots, presented as both two-dimensional (2D) contour plots and three-dimensional (3D) surface plots, as shown in Figure 7. Based on the polynomial model from Equation 4, the 3D surface plots were generated by analyzing the combined influence of two factors at a time, with the third factor maintained at its mid-level value. The color gradients in the plots, ranging from red to green to blue, represent the highest, moderate, and lowest levels of Pb(II) ion rejection, respectively.

The CCD-RSM surfaces and contour plots (Figures 8a-d) show a single broad optimum for Pb(II) rejection (R1) as a quadratic function of feed concentration (A), pressure (B), and pH (C). Along the A-B plane (Fig. 8a and 8c), rejection rose when concentration increased from 60 to 135 ppm and pressure from 1.6 to 2.0 bar, reaching a predicted maximum of ~82% at A=135 ppm and B=2.0 bar, after which R1 declined towards the design-space edges. The initial increase reflected stronger electrostatic exclusion and favorable convective transport at moderate loading, whereas the downturn at higher A and/ or B was consistent with concentration-polarization/fouling that diminished the effective driving force and apparent selectivity (Bowen & Mohammad, 1998; Donnan, 1995; Tsuru et al., 1991; Abdullah et al., 2018; Qadir et al., 2017). On the A-C plane (Figures 8b and 8d), rejection improved with increasing alkalinity and peaked at a pH of approximately 11 at a feed concentration of A = 135 ppm, attributable to the deprotonation of surface groups on the JPU/CDs and enhanced electrostatic repulsion of Pb(II). At lower pH, protonation screens charge and reduces Donnan exclusion (Elimelech & Childress, 1996; Marecka-Migacz et al., 2020). These interactions highlight that moderate concentration, moderate pressure, and mildly alkaline conditions acted synergistically, whereas pushing any factor

to extremes triggered polarization/compaction consequences (Amin et al., 2011; Jamalludin et al., 2021; Yaroshchuk, 2008).

RSM optimization predicted an optimum Pb(II) rejection of around 82% for the JPU/CDs (0.65 wt% CDs) at A = 135 ppm, B = 2 bar, and C = pH 11. Relative to pristine JPU (33% rejection), the incorporation of CDs elevated performance to the 80% class under these operating conditions, confirming the efficacy of the carbon-dot modification.

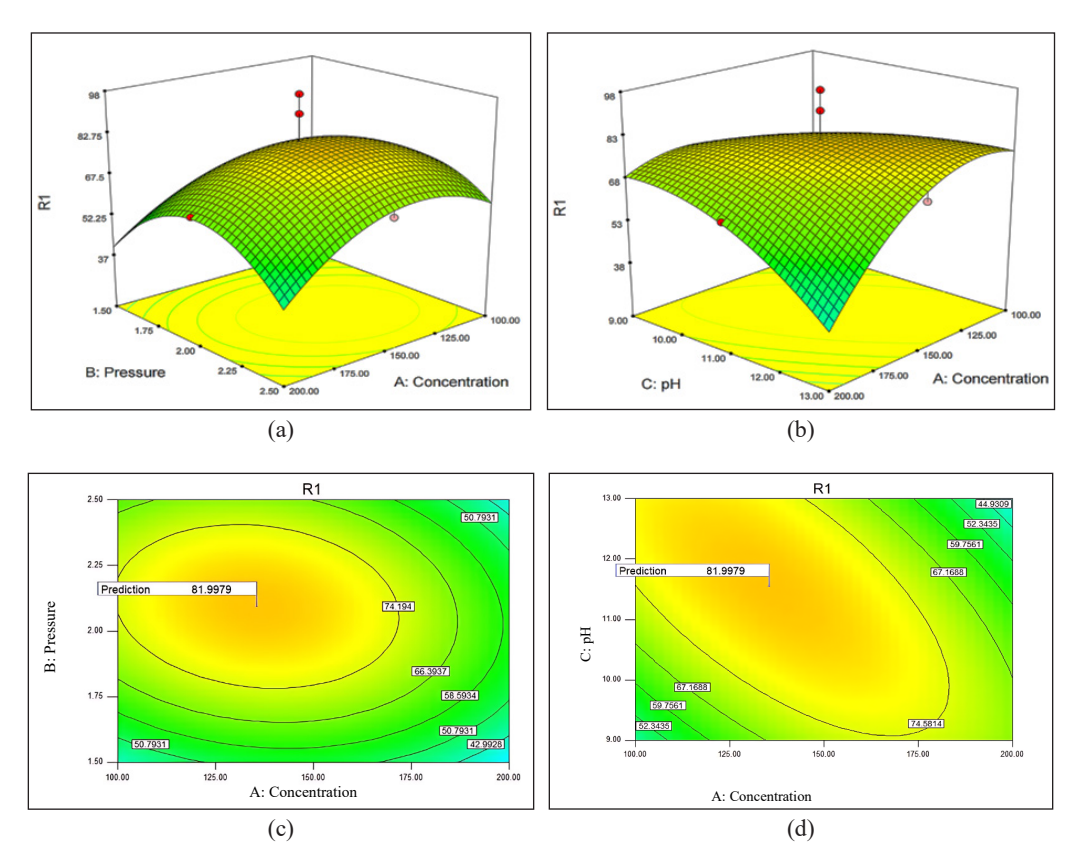


Figure 8. Response-surface (a, b) and contour (c, d) plots for Pb(II) rejection (R1) by JPU/CDs (0.65 wt% CDs): (a, c) concentration–pressure (A–B) interaction and (b, d) concentration–pH (A–C) interaction. A dome-shaped optimum occurs near A = 135 ppm, B = 2.0 bar, and C = pH 11 (predicted R1 = 82%)

Note. JPU = Jatropha polyurethane; CDs = Carbon dots; A = Concentration; B = Pressure; C = pH; CCD = Central composite design, RSM = Response surface methodology

Optimization and Model Validation

The optimization aims to maximize the Pb(II) ions rejection at the suggested conditions. Based on the results obtained, the optimum condition was proposed at 135 ppm, 2 bar, and at pH 11 to obtain the maximum Pb(II) ions rejection (82%), based on the desirability function of 0.8, which indicates the reasonable approximation of the prediction point.

However, in an actual filtration process, JPU/CDs 0.65 wt% replicated with the same optimum condition showed a 67% rejection with 18% error. Pb(II) rejection performance is fairly good compared to the others.

Table 5 compares the filtration performance of pristine JPU, JPU modified with 0.50 wt% GO, and JPU blended with 0.65 wt% CDs. In terms of water permeability, the CD-modified membrane shows a step-change with its preliminary water flux of 873 L/m².h, which is almost 4 times that of pristine JPU (223 L/m².h) and 1.7 times that of the GO composite (523 L/m².h). The likely reason is that the nano-sized CDs create additional porosity and hydrophilic nano-channels, reducing hydraulic resistance. By contrast, the GO membrane more than doubles the pristine flux (+135 %, from 223 to 523 L/m².h); its plate-like sheets introduce hydrophilic pathways but also increase tortuosity, so the permeability boost is significant but not as dramatic as with CDs (Harun et al., 2020).

For heavy metals removal applications, the GO composite delivers the highest selectivity of 71.6 % in the preliminary test for copper ions (Cu^{2+}) removal, rising to 82 \pm 6% after optimization (Harun et al., 2022). In this study, the CD membrane targets Pb²⁺ and achieves 69% rejection in the preliminary run and 67 \pm 18% under optimized conditions, which is roughly double the performance of pristine JPU (33%), but 15% below the GO membrane. Direct quantitative comparison is limited by the different target ions (Cu^{2+} vs. Pb^{2+}), yet the data still illustrate the contrasting strengths of each nanofiller.

With its much higher flux (767 L/m² h at optimum) and moderate Pb²+ rejection, the CD membrane offers the greatest treated-water throughput, which is advantageous for high-flow applications or a multi-stage polishing strategy. The GO membrane appeared to excel in rejection and is therefore better suited to single-stage operations for application with stringent heavy-metal limits. In summary, nanoparticle functionalization is essential for upgrading JPU membranes.

Table 5
Filtration performance of pristine jatropha polyurethane (JPU), JPU with graphene oxide (GO), and JPU with carbon dots (CDs)

	Unmodified pristine JPU	Modified JPU with 0.50% wt GO	JPU/CDs with 0.65wt% CDs (this study)
Preliminary water flux (L/m².h)	2231	5231	873
Preliminary heavy metal rejection (%)	331	71.61	69
Heavy metal rejection % and flux (L/m².h) at	33%1	$87\% (\pm 6\% \text{ error})^2$	67% (± 18% error)
optimum conditions	223 L/m ² .h	Not mentioned ²	767 L/m ² .h

Note. ¹ Harun et al. (2020); ² Harun et al. (2022)

Other studies on the implementation of RSM for nanomaterial-incorporated membranes in filtration have demonstrated varying levels of heavy metal rejection. For instance, an optimized metal oxide membrane incorporated with a nanocomposite achieved a copper ion (Cu(II)) rejection of 49% following RSM optimization (Zahed et al., 2019). Similarly, a polysulfone membrane embedded with cellulose nanofilters exhibited a chromium (VI) ion (Cr(VI)) rejection of 79.85% after optimization through RSM (Gasemloo et al., 2019). Additionally, JPU/GOs membrane filtration, when optimized via RSM, resulted in a Cu(II) rejection of 73.60% while adsorption-based optimization via RSM has demonstrated Pb(II) rejection efficiencies as high as 99% and 92% (Alipour et al., 2020; Harun et al., 2020; Zaferani et al., 2019). Other removal methods, such as cation exchange resin and chemical precipitation, also gave higher removal of Pb(II) at 99% and 97% (Chen et al., 2018; Lalmi et al., 2018). In short, the preliminary Pb(II) rejection performance of JPU/ CD membranes appeared to be relatively lower than other reported methods. Nevertheless, despite the lower rejection efficiency compared to other established methods, JPU/CD membranes still offer potential advantages, such as low cost and sustainability for heavy metal removal, and require further optimization.

CONCLUSION

A regression model was developed based on the experimental design to optimize Pb(II) ion removal efficiency. Under the identified optimal conditions of 135 ppm feed concentration, 2 bar pressure, and pH 11, the model predicted an 82% removal rate. The analysis indicated that lower feed pressure and solution pH had a more pronounced effect on Pb(II) removal, whereas an increase in feed concentration initially enhanced removal efficiency. However, at excessively high feed concentrations, a decline in rejection efficiency was observed, likely due to concentration polarization effects. To refine the predictive accuracy of the model, a reduction approach was applied by eliminating statistically insignificant terms (p > 0.05). The resulting quadratic regression model demonstrated statistical significance, confirming its suitability for optimization predictions. These findings highlight the effectiveness of the developed model in optimizing Pb(II) removal and provide a foundation for further improvements in membrane-based heavy metal remediation strategies.

ACKNOWLEDGEMENTS

We would like to thank the Ministry of Higher Education, Malaysia, under the Fundamental Research Grant Scheme (grant code FRGS/1/2020/TK0/UPM/02/38, project code 03-01-20-2248FR) and the Initiative Putra Grant (GPI/2022/9720400) for their support of this work.

REFERENCES

- Abdullah, N., Rahman, M. A., Othman, M. H. D., Jaafar, J., & Ismail, A. F. (2018). Membranes and membrane processes: Fundamentals. In A. Basile, S. Mozia, R. Molinari (Eds.), Current trends and future developments on (bio-) membranes: Photocatalytic membranes and photocatalytic membrane reactors (pp. 45–70). Elsevier. https://doi.org/10.1016/B978-0-12-813549-5.00002-5
- Abu-Zurayk, R., Alnairat, N., Khalaf, A., Ibrahim, A. A. Halaweh, G. (2023). Cellulose acetate membranes: Fouling types and antifouling strategies A brief review. *Processes*, 11(2), 489. https://doi.org/10.3390/pr11020489
- Alipour, A., Zarinabadi, S., Azimi, A., & Mirzaei, M. (2020). Adsorptive removal of Pb(II) ions from aqueous solutions by thiourea-functionalized magnetic ZnO/nanocellulose composite: Optimization by response surface methodology (RSM). *International Journal of Biological Macromolecules*, 151, 124–135. https://doi.org/10.1016/j.ijbiomac.2020.02.109
- Al-Rashdi, B. A. M., Johnson, D. J., & Hilal, N. (2013). Removal of heavy metal ions by nanofiltration. *Desalination*, 315, 2–17. https://doi.org/10.1016/j.desal.2012.05.022
- Amin, M. M., Hafez, A. I., Shaaban, A. F., Abdelmonem, N. M., & Hanafy, M. (2011). *Removal of reactive dyes from dye-house effluent using nanofiltration membrane*. ResearchGate. https://www.researchgate.net/publication/279297599_Removal_of_Reactive_Dyes_from_Dye-house_Effluent_Using_Nanofiltration_Membrane
- Behera, S. K., Meena, H., Chakraborty, S., & Meikap, B. C. (2018). Application of response surface methodology (RSM) for optimization of leaching parameters for ash reduction from low-grade coal. *International Journal of Mining Science and Technology*, 28(4), 621–629. https://doi.org/10.1016/j.ijmst.2018.04.014
- Bowen, W. R., & Mohammad, A. W. (1998). Characterization and prediction of nanofiltration membrane performance A general assessment. *Chemical Engineering Research and Design*, 76, 885–893. https://doi.org/10.1205/026387698525685
- Chee, D. N. A., Aziz, F., Mohamed Amin, M. A., & Ismail, A. F. (2021). Copper adsorption on ZIF-8/alumina hollow fiber membrane: A response surface methodology analysis. *Arabian Journal for Science and Engineering*, 46, 6775–6786. https://doi.org/10.1007/s13369-021-05636-1
- Chen, Q., Yao, Y., Li, X., Lu, J., Zhou, J., & Huang, Z. (2018). Comparison of heavy metal removals from aqueous solutions by chemical precipitation and characteristics of precipitates. *Journal of Water Process Engineering*, 26, 289–300. https://doi.org/10.1016/j.jwpe.2018.11.003
- Cruz, R., Nisar, M., Palza, H., Yazdani-Pedram, M., Aguilar-Bolados, H., & Quijada, R. (2023). Development of bio degradable nanocomposites based on PLA and functionalized graphene oxide. *Polymer Testing*, 124, 108066. https://doi.org/10.1016/j.polymertesting.2023.108066
- Deshmukh, S. S., & Childress, A. E. (2001). Zeta potential of commercial RO membranes: Influence of source water type and chemistry. *Desalination*, 140(1), 87–95. https://doi.org/10.1016/S0011-9164(01)00357-5
- Donnan, F. G. (1995). Theory of membrane equilibria and membrane potentials in the presence of non-dialysing electrolytes. A contribution to physical-chemical physiology. *Journal of Membrane Science*, 100(1), 45–55. https://doi.org/10.1016/0376-7388(94)00297-C

- Duclos-Orsello, C., Kelly, W., Grant, D. C., Zahka, J., & Thom, V. (2004). Neutral adsorptive capture of particles by membranes: Network modeling near the membrane isoelectric point. *Journal of Membrane Science*, 237(1–2), 167–180. https://doi.org/10.1016/j.memsci.2004.02.030
- Elimelech, M., & Childress, A. E. (1996). Zeta potential of reverse osmosis membranes: Implications for membrane performance. National Technical Reports Library. https://ntrl.ntis.gov/NTRL/dashboard/ searchResults/titleDetail/PB97127450.xhtml
- Emamjomeh, M. M., Torabi, H., Mousazadeh, M., Alijani, M. H., & Gohari, F. (2019). Impact of independent and non-independent parameters on various elements' rejection by nanofiltration employed in groundwater treatment. *Applied Water Science*, *9*, 71. https://doi.org/10.1007/s13201-019-0949-1
- Fang, H., Wang, X., Xia, D., Zhu, J., Yu, W., Su, Y., Zeng, J., Zhang, Y., Lin, X., Lei, Y., & Qiu, J. (2022). Improvement of ecological risk considering heavy metal in soil and groundwater surrounding electroplating factories. *Processes*, 10(7), 1267. https://doi.org/10.3390/pr10071267
- Feng, Z., Adolfsson, K. H., Xu, Y., Fang, H., Hakkarainen, M., & Wu, M. (2021). Carbon dot/polymer nanocomposites: From green synthesis to energy, environmental and biomedical applications. *Sustainable Materials and Technologies*, 29, e00304. https://doi.org/10.1016/j.susmat.2021.e00304
- Gao, F. (2019). An overview of surface-functionalized magnetic nanoparticles: Preparation and application for wastewater treatment. *ChemistrySelect*, 4(22), 6805–6811. https://doi.org/10.1002/slct.201900701
- Gasemloo, S., Khosravi, M., Sohrabi, M. R., Dastmalchi, S., & Gharbani, P. (2019). Response surface methodology (RSM) modeling to improve removal of Cr (VI) ions from tannery wastewater using sulfated carboxymethyl cellulose nanofilter. *Journal of Cleaner Production*, 208, 736–742. https://doi. org/10.1016/j.jclepro.2018.10.177
- Halim, N. A. A., Abidin, Z. Z., Siajam, S. I., Hean, C. G., & Harun, M. R. (2021). Optimization studies and compositional analysis of subcritical water extraction of essential oil from *Citrus hystrix DC*. leaves. *The Journal of Supercritical Fluids*, 178, 105384. https://doi.org/10.1016/j.supflu.2021.105384
- Harun, N. H., Abidin, Z. Z., Abdullah, A. H., & Othaman, R. (2020). Sustainable *Jatropha* oil-based membrane with graphene oxide for potential application in Cu(II) ion removal from aqueous solution. *Processes*, 8(2), 230. https://doi.org/10.3390/pr8020230
- Harun, N. H., Abidin, Z. Z., Majid, U. A., Hamid, M. R. A., Abdullah, A. H., Othaman, R., & Harun, M. Y. (2022). Adopting sustainable *Jatropha* oil bio-based polymer membranes as alternatives for environmental remediation. *Polymers*, 14(16), 3325. https://doi.org/10.3390/polym14163325
- Hu, Q., Yuan, Y., Wu, Z., Lu, H., Li, N., & Zhang, H. (2023). The effect of surficial function groups on the anti-fouling and anti-scaling performance of thin-film composite reverse osmosis membranes. *Journal of Membrane Science*, 668, 121276. https://doi.org/10.1016/j.memsci.2022.121276
- Idress, H., Zaidi, S. Z. J., Sabir, A., Shafiq, M., Khan, R. U., Harito, C., Hassan, S., & Walsh, F. C. (2021).
 Cellulose acetate based complexation-NF membranes for the removal of Pb(II) from waste water. *Scientific Reports*, 11, 1806. https://doi.org/10.1038/s41598-020-80384-0
- Issa, M. A., Abidin, Z. Z., Pudza, M. Y., & Zentou, H. (2020). Efficient removal of Cu(II) from aqueous systems using enhanced quantum yield nitrogen-doped carbon nanodots. RSC Advances, 10(25), 14979–14990. https://doi.org/10.1039/D0RA02276D

- Issa, M. A., Abidin, Z. Z., Sobri, S., Rashid, S. A., Mahdi, M. A., & Ibrahim, N. A. (2020). Fluorescent recognition of Fe³⁺ in acidic environment by enhanced-quantum yield N-doped carbon dots: Optimization of variables using central composite design. *Scientific Reports*, 10, 11710. https://doi.org/10.1038/s41598-020-68390-8
- Jamalludin, M. R., Ahmad Termizi, S. N. A., Khor, C. Y., Hubadillah, S. K., Nawi, M. A. M., Ishak, M. I., & Rosli, M. U. (2021). The modified phase inversion and sintering technique for fabrication of ceramic membrane: Influence of kaolin composition and drying temperature. In AIP Conference Proceedings (Vol. 2339, No. 1, p. 020186). AIP Publishing. https://doi.org/10.1063/5.0044560
- Junker, M. A., Regenspurg, J. A., Valdes Rivera, C. I., te Brinke, E., & de Vos, W. M. (2023). Effects of feed solution pH on polyelectrolyte multilayer nanofiltration membranes. ACS Applied Polymer Materials, 5(1), 355–369. https://doi.org/10.1021/acsapm.2c01542
- Keçili, R., Büyüktiryaki, S., & Hussain, C. M. (2020). Membrane applications of nanomaterials. In C. M. Hussain (Ed.), Handbook of nanomaterials in analytical chemistry: Modern trends in analysis (pp. 159–182). Elsevier. https://doi.org/10.1016/B978-0-12-816699-4.00007-4
- Khamis, F., Hegab, H. M., Banat, F., Arafat, H. A., & Hasan, S. W. (2023). Development of sustainable pH-responsive adsorptive modified mangrove-based polylactic acid ultrafiltration membrane for the removal of heavy metals from aqueous solution. *Chemical Engineering Journal*, 474, 145471. https://doi.org/10.1016/j.cej.2023.145471
- Khdary, N. H., Almuarqab, B. T., & El Enany, G. (2023). Nanoparticle-embedded polymers and their applications: A review. *Membranes*, 13(5), 537. https://doi.org/10.3390/membranes13050537
- Lalmi, A., Bouhidel, K.-E., Sahraoui, B., & el Houda Anfif, C. (2018). Removal of lead from polluted waters using ion exchange resin with Ca(NO₃)₂ for elution. *Hydrometallurgy*, 178, 287–293. https://doi.org/10.1016/j.hydromet.2018.05.009
- Low, K. H., Koki, I. B., Juahir, H., Azid, A., Behkami, S., Ikram, R., Mohammed, H. A., & Md. Zain, S. (2016). Evaluation of water quality variation in lakes, rivers, and ex-mining ponds in Malaysia (review). *Desalination and Water Treatment*, 57(58), 28215–28239. https://doi.org/10.1080/19443994.2016.1185382
- Mamba, F. B., Mbuli, B. S., & Ramontja, J. (2021). Recent advances in biopolymeric membranes towards the removal of emerging organic pollutants from water. *Membranes*, 11(11), 798. https://doi.org/10.3390/ membranes11110798
- Marecka-Migacz, A., Mitkowski, P. T., Nędzarek, A., Różański, J., & Szaferski, W. (2020). Effect of pH on total volume membrane charge density in the nanofiltration of aqueous solutions of nitrate salts of heavy metals. *Membranes*, 10(9), 235. https://doi.org/10.3390/membranes10090235
- Marlina., Farida, M., & Mustanir. (2017). Synthesis and characterization of polyurethane membrane from nyamplung seed oils (*Calophyllum inophillum*). *Asian Journal of Chemistry*, 29(9), 1912–1916. https://doi.org/10.14233/ajchem.2017.20568
- Morales-Jiménez, M., Palacio, D. A., Palencia, M., Meléndrez, M. F., & Rivas, B. L. (2023). Bio-based polymeric membranes: Development and environmental applications. *Membranes*, 13(7), 625. https://doi.org/10.3390/membranes13070625

- Nobre, J. S., & da Motta Singer, J. (2007). Residual analysis for linear mixed models. *Biometrical Journal*, 49(6), 863–875. https://doi.org/10.1002/bimj.200610341
- Petrović, Z. S. (2008). Polyurethanes from vegetable oils. *Polymer Reviews*, 48(1), 109–155. https://doi.org/10.1080/15583720701834224
- Poerio, T., Denisi, T., Mazzei, R., Bazzarelli, F., Piacentini, E., Giorno, L., & Curcio, E. (2022). Identification of fouling mechanisms in cross-flow microfiltration of olive-mills wastewater. *Journal of Water Process Engineering*, 49, 103058. https://doi.org/10.1016/j.jwpe.2022.103058
- Qadir, D., Mukhtar, H. B., & Keong, L. K. (2017). Rejection of divalent ions in commercial tubular membranes: Effect of feed concentration and anion type. Sustainable Environment Research, 27(2), 103–106. https://doi.org/10.1016/j.serj.2016.12.002
- Sgreccia, E., Gonzalez, F. S. G., Prosposito, P., Burratti, L., Sisani, M., Bastianini, M., Knauth, P., & Di Vona, M. L. (2024). Heavy metal detection and removal by composite carbon quantum dots/ionomer membranes. *Membranes*, 14(6), 134. https://doi.org/10.3390/membranes14060134
- Shabbir, H., Csapó, E., & Wojnicki, M. (2023). Carbon quantum dots: The role of surface functional groups and proposed mechanisms for metal ion sensing. *Inorganics*, 11(6), 262. https://doi.org/10.3390/inorganics11060262
- Shi, X., Tal, G., Hankins, N. P., & Gitis, V. (2014). Fouling and cleaning of ultrafiltration membranes: A review. *Journal of Water Process Engineering*, 1, 121–138. https://doi.org/10.1016/j.jwpe.2014.04.003
- Stade, S., Kallioinen, M., Mikkola, A., Tuuva, T., & Mänttäri, M. (2013). Reversible and irreversible compaction of ultrafiltration membranes. Separation and Purification Technology, 118, 127–134. https://doi.org/10.1016/j.seppur.2013.06.039
- Tiwari, A., Pal, D., & Sahu, O. (2017). Recovery of copper from synthetic solution by efficient technology: Membrane separation with response surface methodology. *Resource-Efficient Technologies*, *3*(1), 37–45. https://doi.org/10.1016/j.reffit.2016.12.008
- Tsuru, T., Urairi, M., Nakao, S.-I., & Kimura, S. (1991). Reverse osmosis of single and mixed electrolytes with charged membranes: Experiment and analysis. *Journal of Chemical Engineering of Japan*, 24(4), 518–524.
- van der Kuijp, T. J., Huang, L., & Cherry, C. R. (2013). Health hazards of China's lead-acid battery industry: A review of its market drivers, production processes, and health impacts. *Environmental Health*, *12*, 61. https://doi.org/10.1186/1476-069X-12-61
- Vining, G. (2010). Technical advice: Residual plots to check assumptions. *Quality Engineering*, 23(1), 105–110. https://doi.org/10.1080/08982112.2011.535696
- Wan Yaacob, W. Z., Mohd Pauzi, N. S., & Abdul Mutalib, H. (2009). Acid mine drainage and heavy metals contamination at abandoned and active mine sites in Pahang. *Bulletin of the Geological Society of Malaysia*, 55, 15–20. https://doi.org/10.7186/bgsm55200903
- Xia, C., Ye, H., Wu, Y., AL. Garalleh, H., Garaleh, M., Sharma, A., & Pugazhendhi, A. (2023). Nanofibrous/biopolymeric membrane a sustainable approach to remove organic micropollutants: A review. *Chemosphere*, 314, 137663. https://doi.org/10.1016/j.chemosphere.2022.137663

- Yaroshchuk, A. E. (2008). Negative rejection of ions in pressure-driven membrane processes. *Advances in Colloid and Interface Science*, 139(1–2), 150–173. https://doi.org/10.1016/j.cis.2008.01.004
- Zaferani, S. P. G., Emami, M. R. S., Amiri, M. K., & Binaeian, E. (2019). Optimization of the removal Pb(II) and its Gibbs free energy by thiosemicarbazide modified chitosan using RSM and ANN modeling. *International Journal of Biological Macromolecules*, 139, 307–319. https://doi.org/10.1016/j.ijbiomac.2019.07.208
- Zahed, S. S. H., Khanlari, S., & Mohammadi, T. (2019). Hydrous metal oxide incorporated polyacrylonitrile-based nanocomposite membranes for Cu(II) ions removal. *Separation and Purification Technology*, 213, 151–161. https://doi.org/10.1016/j.seppur.2018.12.027
- Zularisam, A. W., Ismail, A. F., Salim, M. R., Sakinah, M., & Hiroaki, O. (2007). Fabrication, fouling and foulant analyses of asymmetric polysulfone (PSF) ultrafiltration membrane fouled with natural organic matter (NOM) source waters. *Journal of Membrane Science*, 299(1–2), 97–113. https://doi.org/10.1016/j.memsci.2007.04.030